Evaluating forecast baselines and network representativeness for daily $PM_{2.5}$ in the Kathmandu Valley, Nepal

Buddhi Sagar Poudel[1,*], Nita Khatri[2], Namrata Mishra[2], Dhiraj Pradhananga[2]

[1]Nepal Engineering College, Pokhara University, Nepal

[2]Department of Meteorology, Tri-Chandra Multiple Campus, Tribhuvan University, Nepal

* *Corresponding author. Email: iamsagar099@gmail.com*

Peer review status:

This is a non-peer-reviewed preprint submitted to EarthArXiv.

This manuscript has not yet been submitted to a journal for peer review.

Evaluating forecast baselines and network representativeness for daily $PM_{2.5}$ in the Kathmandu Valley, Nepal

Buddhi Sagar Poudel[1,*], Nita Khatri[2], Namrata Mishra[2], Dhiraj Pradhananga[2]

[1]Nepal Engineering College, Pokhara University, Nepal

[2]Department of Meteorology, Tri-Chandra Multiple Campus, Tribhuvan University, Nepal

** Corresponding author. Email: iamsagar099@gmail.com*

Highlights

- Daily PM2.5 is highly coherent across six valley stations (r=0.86, 0.61 anomaly).
- No distance decay is detected within the sampled range; the design can resolve only decay exceeding 0.11-0.21 r-units.
- No fitted model, including tuned random forests, beats an unfitted lag-1 forecast.
- Order-fair attribution: persistence 72%, meteorology 19%, climatology 9%.
- Pooled importance assigns 71% to minimum temperature; this vanishes after deseasonalisation.

Abstract

An order-fair attribution of daily $PM_{2.5}$ predictability in the Kathmandu Valley assigns 72% of achievable error reduction to persistence, 19% to meteorology and 9% to day-of-year climatology, with the latter two largely redundant; no fitted model, including random forests and gradient boosting tuned by nested chronological cross-validation, outperforms an unfitted lag-1 forecast (11.22 μg m^{-3}). We establish this using four years (2021-2024; 5,138 station-days) of daily $PM_{2.5}$, PM_{10} and total suspended particulates from six Department of Environment stations, together with meteorological observations including an hourly 10 m wind record, to test two assumptions common in machine-learning studies of this basin, which report coefficients of determination of 0.80-0.91 pooled across seasons without naive baselines and treat the monitoring network as a set of independent sampling points. Because a three-month season retains a strong sub-seasonal trend, day-to-day relationships are evaluated after removing a day-of-year climatology from both response and predictor, fitted on training data only; confidence intervals account for temporal autocorrelation and for clustering within six stations. Cross-station correlation of daily log $PM_{2.5}$ is 0.86 (95% CI 0.79-0.91), falling to 0.61 (0.52-0.72) after deseasonalisation, with no decay detectable over the 2-13 km network span, though the design resolves only decay larger than 0.11-0.21 r-units. A pooled model attributes 71% of permutation importance to minimum temperature; after deseasonalisation, held-out R^2 falls from 0.64 to 0.10 and that importance disappears. Predictive skill in this basin should be reported against climatology and persistence baselines, and pooled meteorological importances should not be read as physical attribution.

Keywords: $PM_{2.5}$; Kathmandu Valley; spatial representativeness; forecast baselines; persistence; seasonal confounding

1. Introduction

Fine particulate matter is the environmental exposure most consistently associated with premature mortality worldwide, and the burden falls disproportionately on rapidly urbanising cities in South Asia. The Kathmandu Valley, an intermontane basin at roughly 1,300 m enclosed by ridges rising above 2,000 m, combines dense traffic, brick manufacturing, biomass and waste combustion and construction with a topography that restricts ventilation and a monsoon climate that partitions the year into sharply distinct regimes. In the record analysed here, 81.6% of station-days exceed the World Health Organization (2021) daily $PM_{2.5}$ guideline of 15 µg m^{-3} and 16.0% exceed its least stringent interim target of 75 µg m^{-3}; station-year means of 23-73 µg m^{-3} are five to fifteen times the annual guideline.

The valley's seasonal cycle is well documented: a winter and pre-monsoon maximum and a monsoon minimum, attributed to reduced wet deposition, shallow wintertime mixing and topographic trapping (Aryal et al., 2009), and confirmed across in-situ, satellite and reanalysis platforms (Becker et al., 2021). A thermally driven mountain-valley breeze operates on the valley floor with frequent calm conditions in autumn and winter (Pokhrel, 2026), and wintertime source apportionment attributes fine-particle organic carbon largely to garbage burning, biomass burning and fossil fuel (Islam et al., 2022). Predictive modelling is also established: Bhatta and Yang (2023) reconstructed hourly concentrations from 1980 using gradient boosting on a single reference station and reanalysis meteorology, reporting $R^2 \approx 0.84$, and studies combining the national monitoring network with satellite predictors report 0.82-0.84.

Three assumptions underlying this body of work remain untested. First, no study of the basin reports predictive skill against a naive baseline, although a strongly seasonal and strongly autocorrelated series is partly predictable from the date and from its own recent history alone. The consequence is visible in the existing literature: the R^2 reported for this basin can differ substantially between cross-validation and evaluation on genuinely unseen years, because random partitioning of an autocorrelated series places adjacent observations in both training and test sets (Section 4 gives a specific illustration). Naive baselines have been standard in data-driven forecasting since Rasp et al. (2020) but have not been adopted here.

Second, spatial structure in this valley has been characterised for reactive gases rather than particulates. Annual mean NO_2 ranges from 5.7 to 120 ppb across valley sites (Kiros et al., 2016), a twenty-fold range, and land-use regression has been applied to intra-urban NO_2. Whether $PM_{2.5}$ is comparably heterogeneous has not been tested and should not be presumed, since a substantially secondary pollutant with a residence time of days need not share the spatial structure of a primary gas with a lifetime of hours. Third, meteorology-PM associations are conventionally computed within season on raw concentrations, but a three-month season contains a pronounced sub-seasonal trend, so two series that both vary with time of year will correlate even when their day-to-day fluctuations are independent. Removing seasonal structure before examining synoptic-scale relationships is established practice in atmospheric statistics (Leung et al., 2018), where synoptic modes explain 10-40% of daily $PM_{2.5}$ variability in Chinese cities, but is not routine in this regional literature.

We therefore quantify how much independent information the valley monitoring network carries, and how much daily predictability derives from climatology, from autocorrelation and from meteorology when each is measured against explicit naive baselines and under inference appropriate to the data's temporal and spatial dependence.

2. Materials and methods

2.1. Study area and data

The Kathmandu Valley (27.6-27.8°N, 85.2-85.5°E) is an intermontane basin of roughly 650 km^2 with a floor near 1,300 m, enclosed by ridges of 2,000-2,700 m and containing over three million people. Enclosing topography restricts ventilation and promotes nocturnal cold-pool formation in the dry season.

Air-quality data are daily mean $PM_{2.5}$, PM_{10} and total suspended particulates from Department of Environment stations, 1 January 2021 to 31 December 2024 (Table 1, Fig. 1). Meteorological data are Department of Hydrology and Meteorology daily temperature extremes, precipitation and relative humidity, and hourly 10 m wind speed and direction. Two air-quality sites are effectively co-located with wind stations (Kirtipur, 0.04 km; Khumaltar, 0.60 km); elsewhere meteorological values are spatial proxies, and pairing distance is retained for sensitivity analysis. Station identifiers, which differ across annual releases and between agencies, were harmonised against station coordinates and verified numerically; details are in Supplementary Material S1. Meteorological timestamps are UTC and were converted to Nepal Standard Time (UTC+05:45) before daily aggregation. Precipitation recorded at 08:45 local time is the 24-hour accumulation ending that morning, and lagged analyses account for this offset.

Missingness is structural, reflecting station commissioning and decommissioning rather than sporadic dropout, with multi-year gaps at two sites (Table 2). We therefore use complete-case analysis and do not impute $PM_{2.5}$, since imputation to a complete panel would fabricate station-years and confound estimates with changing network composition. One site operated for 179 days in a single year and is excluded, leaving six stations and 5,138 station-days with valid $PM_{2.5}$. Physical ordering violations among the three size fractions were rare (<0.5%), were retained, and their exclusion does not affect any conclusion. One automatic weather station reporting 12.6% exact zero wind speeds, an instrument threshold artefact, is excluded from calm-hour statistics.

Table 1. Data sources, variables and coverage over 2021-2024.

Source	Variable	Resolution	Sites used	Present
DoE	PM2.5	Daily	6	5,138 station-days
DoE	PM10	Daily	6	5,176
DoE	TSP	Daily	5	3,767
DHM	Maximum / minimum temperature	Daily	9	99.0 / 97.7 %
DHM	Precipitation	Daily	15	98.3 %
DHM	Relative humidity	Daily	9	100 %
DHM	Wind speed and direction, 10 m	Hourly	5	85.1 % (daily aggregates)

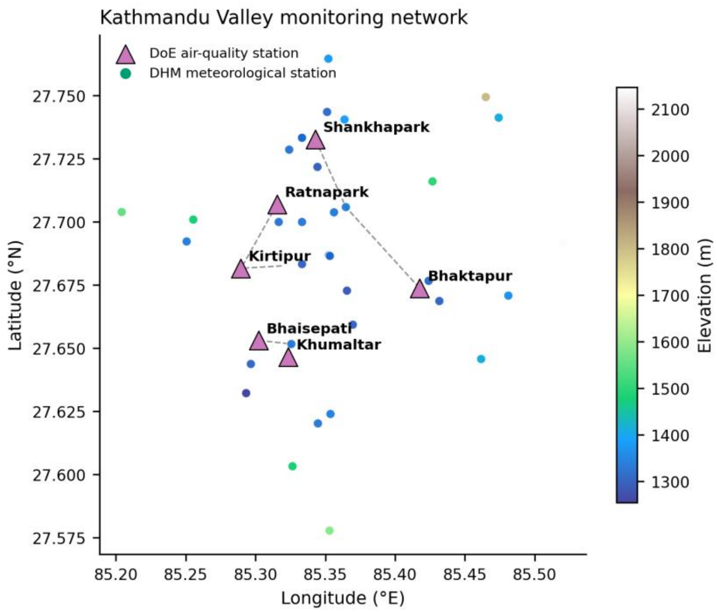

Fig. 1. The Kathmandu Valley monitoring network. Triangles mark air-quality stations, circles mark meteorological stations coloured by elevation, and dashed lines join each air-quality site to its paired wind station. All six air-quality sites lie on the valley floor within an 11 km span.

2.2. Deseasonalisation

Seasons follow the convention standard for the Nepali climate: winter (December-February), pre-monsoon (March-May), monsoon (June-September) and post-monsoon (October-November). Where a claim concerns day-to-day behaviour, a K-harmonic day-of-year climatology f_s is removed from both response and predictor, separately for each station s, giving anomalies $y'_{s,t} = y_{s,t} - f_s(d(t))$ for day-of-year $d(t)$.

In every out-of-sample experiment f_s is estimated on the training period alone and applied unchanged to the test period. Raw and anomaly results are reported in parallel because they answer different questions: meteorology drives the annual cycle, and the anomaly analysis isolates whether it also carries information about departures from that cycle. The main text uses K=4; sensitivity to K=1-6 is reported in Section 3.6.

2.3. Statistical inference

Confidence intervals account for temporal autocorrelation by moving-block bootstrap (Künsch, 1989), resampling contiguous blocks jointly across stations (30 days for correlations, 14 for forecast skill). Because cluster-robust standard errors are unreliable with few clusters (Cameron et al., 2008; MacKinnon and Webb, 2017), tests of the season × meteorology interaction use a wild cluster bootstrap with Rademacher weights; six clusters admit only $2^6=64$ sign vectors, so the distribution is enumerated exactly, which imposes a resolution floor of $p=0.016$. Spearman rank correlation is used for monotone association, Kruskal-Wallis for multi-group comparison, and analyses are performed on log-transformed concentrations. Effect sizes with intervals are reported in preference to p-values throughout.

2.4. Models and validation

Modelling isolates the contribution of each information source rather than comparing algorithms. A nested sequence adds day-of-year climatology, meteorology and $PM_{2.5}$ persistence (lags 1-3 and a lagged three-day mean) to a station-mean baseline, and each configuration is fitted with linear regression, ridge, random forest (Breiman, 2001) and gradient boosting, then compared against an unfitted lag-1 persistence forecast. Because sequential decomposition assigns to each source only the variance not already claimed by earlier entrants, and climatology and meteorology are mutually redundant, we also report an order-fair Shapley attribution: each source's marginal contribution averaged over all 3!=6 entry orders (Shapley, 1953), requiring all 2^3 information subsets. A further configuration substitutes the neighbouring stations' mean concentration on the previous day for meteorology, testing whether spatial coherence supplies information beyond a station's own history.

Validation is chronological throughout; no random splitting is used at any stage. The primary split trains on 2021-2023 and tests on 2024, and confirmatory results use rolling-origin expanding-window validation with six-month steps. Lags are within-station and past-only, and climatology is fitted on training data alone. Random-forest and boosting hyperparameters are selected by grid search under an inner four-fold TimeSeriesSplit on the training period, with the selected configuration refitted and evaluated once on the held-out year (Table 5). No same-day PM_{10} or TSP is used to predict $PM_{2.5}$, since these correlate at $r=0.92$ and their inclusion would constitute contemporaneous regression rather than forecasting. Network subset selection is likewise performed on the training period and evaluated on the held-out year.

Pre-specified sensitivity analyses comprise alternative meteorological pairing, restriction to sub-kilometre wind pairings, leave-one-station-out and leave-one-year-out, alternative season definitions, alternative episode thresholds (85th, 90th, 95th percentiles) and deseasonalisation order K=1-6.

3. Results

3.1. Data characteristics

The analysis dataset comprises 5,138 station-days with valid $PM_{2.5}$, 5,176 with PM_{10} and 3,767 with TSP over 1,461 days. Coverage is uneven (Table 2): only two stations span all four years, at 78.8% and 66.5% of possible days, while the least complete reaches 32.2% and contains an 823-day gap. Meteorological coverage after harmonisation is 99.0% for maximum temperature, 98.3% for precipitation, 100% for relative humidity and 85.1% for daily wind aggregates.

Table 2. Station characteristics and coverage, 2021-2024 (1,461 possible days each). Concentrations in µg m-3.

Station	**Lat (°N)**	**Lon (°E)**	**n**	**Coverage**	**Largest gap**	**Median**	**p95**	**Wind pairing**
Ratnapark	27.7070	85.3154	1,151	78.8 %	68 d	38.5	97.7	3.8 km
Kirtipur	27.6817	85.2893	972	66.5 %	106 d	39.9	96.9	0.04 km
Khumaltar	27.6466	85.3234	949	65.0 %	21 d	41.4	89.5	0.60 km
Bhaisepati	27.6531	85.3023	736	50.4 %	397 d	34.4	124.0	2.3 km

Station	Lat (°N)	Lon (°E)	n	Coverage	Largest gap	Median	p95	Wind pairing
Shankhapark	27.7328	85.3428	681	46.6 %	25 d	43.0	85.5	3.7 km
Bhaktapur	27.6738	85.4175	470	32.2 %	823 d	47.5	100.4	6.3 km

3.2. Spatial coherence

Daily log $PM_{2.5}$ is strongly correlated across the network, with a mean pairwise coefficient of 0.856 (95% CI 0.787-0.909; range 0.73-0.97). Removing the annual cycle reduces this to 0.610 (0.516-0.721), retaining 71% of the raw value, so coherence is not an artefact of shared seasonality (Fig. 2a).

Correlation shows no relationship with inter-station separation: on raw values the slope is −0.0010 r-units km^{-1} (95% CI −0.0131 to +0.0074; permutation p=0.91) and on anomalies +0.0043 (−0.0165 to +0.0222; p=0.75), with leave-one-pair-out slopes confirming that no single pair drives the result. These intervals imply that the design resolves only a decay exceeding roughly 0.010-0.019 r-units km^{-1}, that is 0.11-0.21 r-units across the network's 11 km span; a smaller genuine decay would not be detected, and we therefore report an absence of detectable decay within the sampled range rather than evidence that the valley constitutes a single airshed.

A single station reproduces the mean of all others with R^2=0.938 on raw values and 0.780 on anomalies, computed leave-one-out so that the target excludes the predictor (Fig. 2b). One station departs from this pattern: the city-centre roadside site has the network's lowest anomaly correlations (0.34-0.63) and a reconstruction R^2 of only 0.353, a distinct local signal consistent with the traffic-linked spatial heterogeneity documented for NO_2 here (Kiros et al., 2016). Selecting the best station subset on 2021-2023 and evaluating it on 2024 gives R^2=0.699 for one station and 0.707 for three, against in-sample values above 0.98; four and five stations reach 0.938 and 0.980 (Fig. 6b). In-sample selection therefore substantially overstates what a reduced network would achieve.

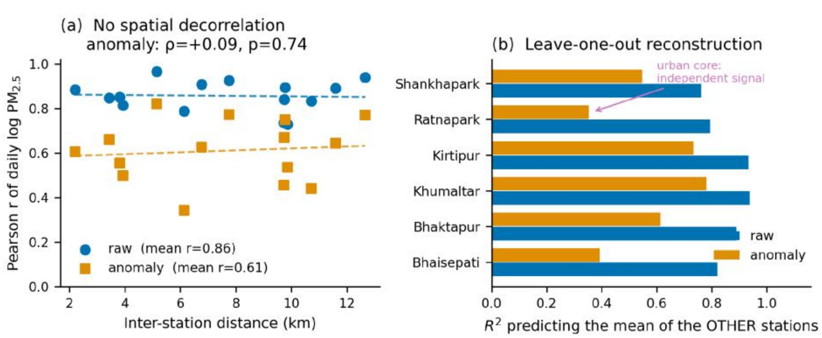

Fig. 2. Spatial coherence of daily PM2.5. (a) Pairwise correlation against inter-station distance for raw log concentrations (circles) and deseasonalised anomalies (squares), with least-squares fits. (b) Leave-one-out reconstruction: the coefficient of determination when each station predicts the mean of all other stations.

3.3. Seasonal structure and episodes

Winter and pre-monsoon have almost identical mean concentrations, 64.7 and 64.1 μg m^{-3}, but markedly different dispersion: standard deviations of 22.0 and 32.4 and 95th percentiles of 99.1 and 123.1 (Table 3). Consistent with this, 63.4% of station-specific 90th-percentile exceedance days fall in the pre-monsoon and only 34.8% in winter (Fig. 3). Winter is better described as a high, stable plateau, with the pre-monsoon generating the extremes, a distinction relevant to exposure assessment and not emphasised in the existing literature, which generally identifies winter as the pollution season.

Episodes are predominantly multi-day: 177 network-wide, with 70% of exceedance days occurring in runs of three days or longer and a maximum run of 16 days. The fine fraction declines in the pre-monsoon at five of six stations and differs significantly across seasons (Kruskal-Wallis H=255.1, $p=5\times10^{-55}$) and stations (H=421.4, $p=7\times10^{-89}$). Coarse-particle enrichment during pre-monsoon episodes is consistent with dust, resuspension or biomass burning, but without chemical speciation these cannot be distinguished and we do not attribute them.

The hourly wind record shows a thermally driven valley circulation with a diurnal amplitude of 2.12 and 2.06 m s^{-1} at the two valley-floor sites, peaking near 15:00 local time, against 0.46 m s^{-1} at a rim site 800 m higher (Supplementary Fig. S2), an observational signature of a shallow boundary layer decoupling the valley floor from the free atmosphere. Wind speeds are low throughout, with a median daily mean near 1.0 m s^{-1} and monthly means spanning only 1.0-1.5 m s^{-1}.

Table 3. PM2.5 descriptive statistics by season (µg m-3), all stations pooled.

Season	n	Mean	SD	25th	Median	75th	95th	Max
Winter (DJF)	1,143	64.7	22.0	51.3	63.1	77.1	99.1	215.0
Pre-monsoon (MAM)	1,410	64.1	32.4	40.6	58.7	81.5	123.1	238.3
Monsoon (JJAS)	1,614	18.9	11.8	11.5	15.2	21.9	43.7	133.3
Post-monsoon (ON)	792	35.5	16.1	23.4	33.3	46.1	63.5	96.3

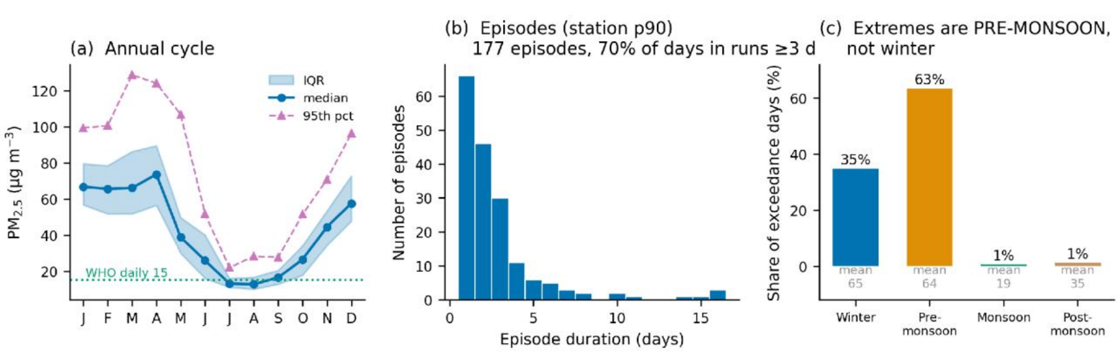

Fig. 3. Seasonal and episodic structure. (a) Monthly climatology: median, interquartile range and 95th percentile, with the WHO daily guideline marked. (b) Episode durations, an episode being a run of consecutive days above that station's 90th percentile. (c) Share of exceedance days by season, with seasonal mean annotated.

3.4. Meteorological associations and their seasonal stability

Pooled across seasons, $PM_{2.5}$ shows the associations typically reported for this basin: Spearman ρ of −0.68 with minimum temperature, −0.57 with precipitation, −0.53 with relative humidity and +0.64 with diurnal temperature range. Removing the annual cycle from both sides changes this substantially (Table 4): monsoon humidity falls from −0.34 to −0.09 and post-monsoon minimum temperature from −0.46 to +0.02, a reversal of sign, while pre-monsoon humidity is the principal survivor at −0.34 and precipitation retains a consistent −0.16 to −0.20 in every non-winter season, the expected wet-deposition signal.

Meteorological sensitivity does not differ significantly between seasons once inference accounts for the six-station clustering. On raw values the four season × meteorology interaction terms are large (0.29-0.68 log units per standard deviation) but reach only p=0.016-0.031 under wild cluster bootstrap, at or near the 1/64 floor imposed by six clusters; on anomalies the terms shrink to 0.03-0.09 and none is significant (p=0.078-0.375). The apparent seasonal contrast on raw values is therefore substantially a sub-seasonal trend confound, a winter plateau compared against transition seasons containing steep within-season trends. Full coefficients are given in Supplementary Table S5.

Table 4. Spearman correlation between PM2.5 and surface meteorology by season, shown as raw → anomaly (K=4). n ranges from 611 to 1,701 station-days per season.

Variable	Winter	Pre-monsoon	Monsoon	Post-monsoon
Relative humidity	−0.01 → +0.07	−0.38 → −0.34	−0.34 → −0.09	−0.13 → −0.03
Diurnal temperature range	−0.12 → −0.13	+0.41 → +0.24	+0.35 → +0.23	+0.24 → −0.04
Minimum temperature	+0.10 → +0.20	−0.30 → +0.03	−0.19 → −0.06	−0.46 → +0.02
Maximum temperature	−0.05 → +0.04	+0.11 → +0.33	+0.26 → +0.18	−0.44 → −0.06
Precipitation	−0.08 → −0.02	−0.47 → −0.18	−0.31 → −0.16	−0.45 → −0.20
Wind speed (daily mean)	−0.16 → −0.10	−0.02 → −0.08	+0.11 → −0.04	−0.13 → +0.05
Wind speed (afternoon)	−0.12 → −0.08	+0.18 → +0.06	+0.16 → +0.01	−0.01 → +0.06

3.5. Sources of daily predictability

An unfitted lag-1 persistence forecast, where today's prediction is yesterday's measurement, attains a test RMSE of 11.22 μg m^{-3} on the 2024 test set. No fitted model improves on it: ridge reaches 11.38, linear regression 11.43, a random forest tuned by nested chronological cross-validation 11.51 and tuned gradient boosting 12.21 (Table 5). Tuning matters, as it improves the random forest from 11.77 and boosting from 13.84, but does not close the gap. Applying the moving-block bootstrap to the model-baseline difference gives intervals that all straddle zero (+0.44 μg m^{-3}, 95% CI −0.12 to +0.91 for the persistence random forest; +0.37, −0.71 to +1.15 for the full model), with fitted models outperforming the baseline on 5-20%

of resamples. The defensible claim is that no fitted model, including tuned random forests and gradient boosting, outperforms an unfitted lag-1 forecast, rather than that the one-liner wins.

Entering information in the conventional order, knowing only the date reduces RMSE by 28.5% relative to a station mean, adding meteorology adds 2.2%, and adding recent concentration history instead adds 49.7%, reaching R^2=0.847. This decomposition is order-dependent, and the conventional order is not neutral: meteorology receives 2.2% entering after climatology but 10.75 µg m^{-3} of error reduction entering first, and 0.08 entering last. Meteorology alone (RMSE 22.64) in fact outperforms day-of-year climatology alone (26.78); both encode season, so whichever enters first absorbs the shared contribution. Averaging over all six entry orders gives persistence 15.36 µg m^{-3} (71.6%), meteorology 4.08 (19.0%) and day-of-year climatology 2.01 (9.4%) (Fig. 4). Meteorology's share is therefore approximately 19%, not the 2% the sequential split implies, while persistence dominates by a factor of nearly four regardless of ordering.

Adding meteorology to persistence changes RMSE by +0.7% with a 90% interval of [−4.4%, +7.5%], which excludes effects larger than about ±10% but not effects within ±5%; the incremental contribution is thus inconclusive rather than absent. Under rolling-origin validation the per-fold increments span −0.7 to +14.8%, giving a between-fold interval of [−3.96%, +11.66%] that overlaps the within-year interval and likewise includes zero. Substituting the neighbouring stations' previous-day mean for meteorology gives an increment of −0.30% (95% CI −1.28 to +0.74); used alone it reaches RMSE 25.26, close to meteorology alone at 25.77. High spatial coherence therefore means that neighbouring stations carry the same information as a station's own recent history, not additional information.

Table 5. Test RMSE (µg m-3) on the chronological 2024 test set (n=848 station-days; trained on 2021-2023). Upper block: sequential nested decomposition, untuned, common sample. Lower rows: full information set with hyperparameters selected by inner TimeSeriesSplit cross-validation on the training period alone.

Information / model	**Linear**	**Random forest**	**Gradient boosting**
Station mean only	—	33.18	—
+ day-of-year climatology	23.74	23.74	23.74
+ meteorology	22.83	23.21	23.74
+ PM2.5 persistence	11.37	11.66	14.37
+ meteorology + persistence	11.38	11.74	13.45
Full set, tuned	11.38 †	11.51	12.21
Lag-1 persistence (no fitted model)	—	11.22	—

† Ridge with α selected by inner cross-validation. Selected hyperparameters: random forest depth 8, minimum leaf 10, all features; boosting depth 3, learning rate 0.03, L2 penalty 5.

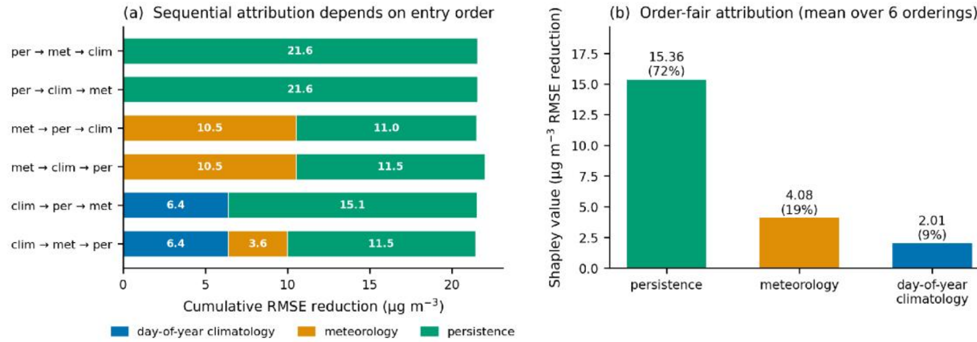

Fig. 4. Attribution of predictive information. (a) Sequential decomposition under each of the six entry orders; the share assigned to meteorology and to climatology depends strongly on which enters first. (b) Order-fair attribution averaging marginal contributions over all orderings.

3.6. Feature importance, sensitivity and robustness

A pooled random forest with ten meteorological predictors attains held-out R^2=0.644 and attributes 71% of permutation importance to minimum temperature (0.569, 95% range across seeds 0.549-0.584), followed by relative humidity at 11.5% (Fig. 5a). Repeating the procedure on anomalies, with the climatology fitted on training data only, held-out R^2 falls to 0.102 and the importance of minimum temperature to −0.004±0.004 (Fig. 5b). Minimum temperature functions substantially as a calendar variable, tracking the annual cycle as $PM_{2.5}$ does. Residual skill is small but not zero, and part of it may be seasonality that a training-period climatology does not fully capture, so the defensible statement is that day-to-day meteorological information is roughly an order of magnitude smaller than the pooled model implies.

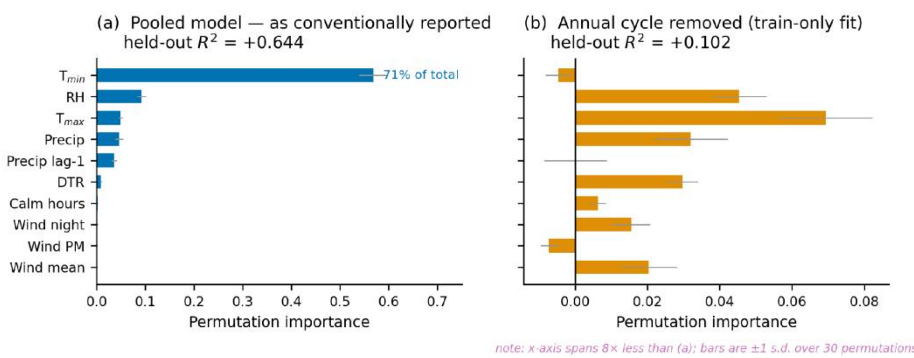

Fig. 5. Meteorological attribution before and after removing the annual cycle. (a) Permutation importance from a pooled model. (b) The identical procedure on anomalies, with the climatology fitted on training data only. Bars are ±1 standard deviation over 30 permutations; the horizontal axis in (b) spans far less than in (a).

Spatial conclusions are stable across deseasonalisation order, with mean pairwise anomaly correlation ranging only 0.61-0.68 and the distance association negligible throughout; the anomaly-model skill estimate is less stable, ranging 0.04-0.28 across K=1-6, and is reported as a range for that reason (Fig. 6a). Substituting a single valley reference station for the variable-specific meteorological pairing, restricting wind analyses to the two sub-kilometre pairings, omitting each station and each year in turn, excluding ordering-violation records, and varying episode thresholds all leave the reported conclusions unchanged in direction and approximate magnitude.

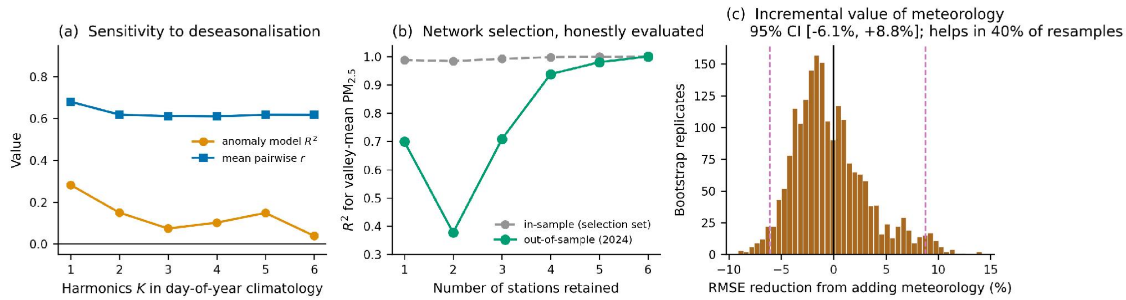

Fig. 6. Uncertainty and sensitivity. (a) Dependence of anomaly-model skill and mean pairwise anomaly correlation on the number of harmonics. (b) Network subset selection evaluated in-sample (grey) and out-of-sample (green). (c) Bootstrap distribution of the error reduction obtained by adding meteorology to persistence.

3.7. Multi-day forecast horizons

We repeated the Section 3.5 comparison at forecast horizons of k = 1, 2, 3 and 7 days on the same chronological 2024 test set, retuning hyperparameters at each horizon by inner TimeSeriesSplit cross-validation on the training period. Two settings were considered: meteorology lagged by k days, which is operationally realistic, and target-day meteorology supplied directly, an upper bound corresponding to a perfect weather forecast.

No model outperformed lag-k persistence at any horizon tested, in either setting (Fig. 7). All bootstrap intervals for the model-minus-persistence RMSE difference crossed zero, and the probability that a fitted model beat the baseline on a resample never exceeded 0.72 (ridge, k = 2, lagged meteorology) and was usually at or below 0.5. Random forest and gradient boosting were consistently worse than persistence beyond k = 1, including under perfect prognosis. Persistence RMSE increased from 11.2 to 19.8 µg m^{-3} between k = 1 and k = 7, a rate matched or exceeded by every fitted model; day-of-year climatology alone remained flat near 23.5-23.8 µg m^{-3} at every horizon and was outperformed by persistence throughout. The persistence dominance reported in Section 3.5 therefore extends across the week rather than being specific to the one-day horizon.

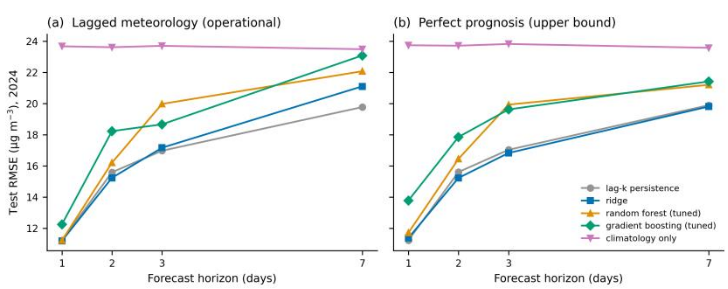

Fig. 7. Forecast RMSE by horizon, 2024 test set. (a) Meteorology lagged by k days (operational setting). (b) Target-day meteorology supplied directly (perfect-prognosis upper bound). No fitted model improves on lag-k persistence at any tested horizon in either setting.

4. Discussion

Daily $PM_{2.5}$ in this basin is organised by a small number of information sources with very unequal weight. Autocorrelation dominates, taking roughly seventy per cent of achievable error reduction under an order-fair attribution, and no fitted model improves on using the previous day's measurement directly. Seasonal structure takes most of the remainder, shared between meteorology and the calendar, which are largely redundant with one another. Spatial position contributes little: station identity accounts for 3.0% of variance, and neighbouring stations supply no information beyond a station's own history. What remains is a substantial, autocorrelated residual that this design cannot attribute.

The dominance of persistence is best read as an accumulation signature. Concentrations in an enclosed basin with weak ventilation reflect a slowly evolving reservoir rather than a rapidly flushed one, so today's burden is largely yesterday's modified at the margin. The episode structure supports this, with seventy per cent of exceedance days falling in runs of three days or longer and runs extending to sixteen days.

These results do not imply that meteorology is unimportant. Under order-fair attribution it accounts for roughly a fifth of achievable error reduction, and it plainly governs the annual cycle: the monsoon minimum is a wet-deposition phenomenon, precipitation retains a consistent negative anomaly association outside winter, and pre-monsoon humidity retains most of its raw association after deseasonalisation. The defensible statement is that meteorology carries substantial seasonal information, largely redundant with the calendar, and an incremental day-to-day contribution beyond persistence that this design cannot resolve. Two features of the basin plausibly explain the latter: the dynamic range of ventilation is small, with monthly mean wind spanning only 1.0-1.5 m s^{-1}, and a variable that barely varies cannot explain variation elsewhere; and the enclosing topography that produces the pollution problem also suppresses synoptic influence at the valley floor, as the near-absence of a diurnal cycle at the rim indicates. In open terrain, where synoptic systems modulate ventilation across a wide range, surface meteorology would be expected to carry considerably more day-to-day information, consistent with the 10-40% of daily variability attributed to synoptic modes in Chinese cities (Leung et al., 2018).

Our seasonal climatology agrees with the established literature, and our skill (R^2=0.847) is consistent with the 0.80-0.91 range previously reported; the contribution is not a higher number but an account of where it originates, and the demonstration that an unfitted persistence forecast matches it. Bhatta and Yang (2023) report a strong $PM_{2.5}$-humidity anti-correlation, which we reproduce pooled and additionally show does not survive deseasonalisation outside the pre-monsoon, which is not a contradiction, since the pooled relationship is the mechanism by which meteorology sets the seasonal cycle. Bhatta and Yang (2023) illustrate the value of the baseline comparison advocated here: their reported R^2 of 0.84, obtained under ten-fold cross-validation, fell to 0.56-0.67 when the same model was evaluated on genuinely unseen years, the discrepancy random k-fold partitioning of an autocorrelated series produces. On spatial structure our result contrasts with the twenty-fold NO_2 range documented by Kiros et al. (2016), a contrast that is physically coherent: NO_2 is primary with a lifetime of hours, so concentrations track proximity to emission, whereas $PM_{2.5}$ here has a substantial secondary and transported component and a residence time of days. That the roadside site is the one station retaining an independent signal supports this reading.

Three consequences follow. Predictive skill in this basin should be reported against both a day-of-year climatology and a persistence baseline under chronological validation, since a model reporting R^2=0.85 without them is principally reporting that it has learned the annual cycle and the autocorrelation, a claim a one-line forecast also satisfies. Meteorological feature importances from pooled models should be checked against a deseasonalised comparison before being interpreted physically, since the procedure that assigns 71% of importance to minimum temperature assigns it essentially none once the annual cycle is removed. And within the spatial envelope this network samples, additional stations measuring the shared signal add limited information, while the roadside site demonstrably carries a distinct one; honest out-of-sample figures are more modest than in-sample selection implies, with one station reproducing the valley mean at $R^2 \approx 0.70$ and four to five required to exceed 0.93. This suggests that temporal continuity and site diversity may yield greater marginal information than further replication of similar valley-floor sites.

Several limitations bound these conclusions. The study is observational and all relationships are associational. Six valley-floor stations within an 11 km span cannot characterise the valley margins, other elevations or areas outside that envelope, and the design resolves only distance decay exceeding 0.11-0.21 r-units; inference rests on six clusters, capping attainable significance at p=0.016. Daily resolution limits mechanistic inference, since inversion breakup and combustion cycles operate sub-daily, and no chemical speciation is available to attribute coarse-fraction changes to a source. The station panel is unbalanced, meteorological values outside two sites are spatial proxies, and absent instrument metadata, apparent between-year shifts cannot be separated from instrument changes. Four years is short and we make no trend claim. Results are specific to a topographically enclosed basin.

After removing the annual cycle, day-to-day variability remains substantial (anomaly standard deviation ≈ 0.41 in log units, roughly ±50%) and strongly autocorrelated, yet is only weakly predicted out-of-sample by surface meteorology. Candidate explanations this design cannot separate include day-to-day emission variability, in-valley boundary-layer processes and regional transport; a preliminary analysis using reanalysis boundary-layer fields is reported in Supplementary Material S3, but the reanalysis reproduces in-valley wind at only r=0.30, a resolution at which a null result cannot be interpreted as evidence about mixing depth. Resolving this would require in-valley vertical profiling at sub-daily resolution and a day-resolved emissions inventory, neither of which exists for this period. Deploying two or three stations outside the present spatial envelope would likewise convert the coherence result from a statement about the existing network into a statement about the valley.

5. Conclusions

Using four years of daily particulate measurements from six stations with concurrent meteorological observations, we find that daily $PM_{2.5}$ across the Kathmandu Valley monitoring network is highly spatially coherent, with cross-station correlation of 0.86 falling to 0.61 after the annual cycle is removed and no decay detectable across the 11 km span sampled, and that a single roadside site is the only station carrying a substantially independent signal. Daily predictability is dominated by autocorrelation: an order-fair attribution assigns 72% of achievable error reduction to persistence against 19% for meteorology and

9% for the calendar, and no fitted model, including tuned random forests and gradient boosting, outperforms an unfitted lag-1 forecast.

These findings concern what is learnable at daily resolution beyond the annual cycle, not the well-established role of meteorology in setting that cycle. They imply that predictive skill in this basin should be quoted against climatology and persistence baselines, and that meteorological importances from pooled models require a deseasonalised comparison before physical interpretation. The large, autocorrelated day-to-day variability that remains unexplained is the most useful open problem this dataset identifies.

CRediT authorship contribution statement

Buddhi Sagar Poudel: Conceptualization, Data curation, Formal analysis, Investigation, Methodology, Writing draft.
Nita Khatri: Data curation, editing draft, data preparation, hypothesis testing.
Namrata Mishra: Data curation, editing draft, data preparation, hypothesis testing.
Dhiraj Pradhananga: Supervision, Validation, review & editing.

Declaration of competing interest

The authors declare that they have no known competing financial interests or personal relationships that could have appeared to influence the work reported in this paper.

Data and code availability

Air-quality data are published by the Department of Environment, Government of Nepal; meteorological data are provided by the Department of Hydrology and Meteorology, Government of Nepal. The merged analysis dataset, station crosswalk, and analysis and figure-generation code are archived on Zenodo (https://doi.org/10.5281/zenodo.22148941); files are available on request through the Zenodo platform.

Acknowledgements

The authors thank the Department of Hydrology and Meteorology (DHM) and the Department of Environment (DOE), Government of Nepal, for their support throughout the data collection process.

References

Aryal, R.K., Lee, B.-K., Karki, R., Gurung, A., Kandasamy, J., Pathak, B.K., Sharma, S., Giri, N., 2009. Dynamics of PM2.5 concentrations in Kathmandu Valley, Nepal. Journal of Hazardous Materials 168 (2–3), 732–738.

Becker, S., Sapkota, R.P., Pokharel, B., Adhikari, L., Pokhrel, R.P., Khanal, S., Giri, B., 2021. Particulate matter variability in Kathmandu based on in-situ measurements, remote sensing, and reanalysis data. Atmospheric Research 258, 105623.

Bhatta, S., Yang, Y., 2023. Reconstructing PM2.5 data record for the Kathmandu Valley using a machine learning model. Atmosphere 14 (7), 1073.

Breiman, L., 2001. Random forests. Machine Learning 45 (1), 5–32.

Cameron, A.C., Gelbach, J.B., Miller, D.L., 2008. Bootstrap-based improvements for inference with clustered errors. Review of Economics and Statistics 90 (3), 414–427.

Islam, M.R., Li, T., Mahata, K., Khanal, N., Werden, B., Giordano, M.R., Puppala, S.P., Dhital, N.B., Gurung, A., Saikawa, E., Panday, A.K., Yokelson, R.J., DeCarlo, P.F., Stone, E.A., 2022. Wintertime air quality across the Kathmandu Valley, Nepal: concentration, composition, and sources of fine and coarse particulate matter. ACS Earth and Space Chemistry 6 (12), 2955–2971.

Kiros, F., Shakya, K.M., Rupakheti, M., Regmi, R.P., Maharjan, R., Byanju, R.M., Naja, M., Mahata, K., Kathayat, B., Peltier, R.E., 2016. Variability of anthropogenic gases: nitrogen oxides, sulfur dioxide, ozone and ammonia in Kathmandu Valley, Nepal. Aerosol and Air Quality Research 16 (12), 3088–3101.

Künsch, H.R., 1989. The jackknife and the bootstrap for general stationary observations. Annals of Statistics 17 (3), 1217–1241.

Leung, D.M., Tai, A.P.K., Mickley, L.J., Moch, J.M., van Donkelaar, A., Shen, L., Martin, R.V., 2018. Synoptic meteorological modes of variability for fine particulate matter (PM2.5) air quality in major metropolitan regions of China. Atmospheric Chemistry and Physics 18, 6733–6748.

MacKinnon, J.G., Webb, M.D., 2017. Wild bootstrap inference for wildly different cluster sizes. Journal of Applied Econometrics 32 (2), 233–254.

Pokhrel, R., 2026. Dynamics of air pollution and its dispersion in a topographically constrained urban area: a case study of Kathmandu Valley. Pokhara Engineering College Journal 3 (1), 17–39.

Rasp, S., Dueben, P.D., Scher, S., Weyn, J.A., Mouatadid, S., Thuerey, N., 2020. WeatherBench: a benchmark dataset for data-driven weather forecasting. Journal of Advances in Modeling Earth Systems 12 (11), e2020MS002203.

Shapley, L.S., 1953. A value for n-person games. In: Kuhn, H.W., Tucker, A.W. (Eds.), Contributions to the Theory of Games II. Princeton University Press, Princeton, pp. 307–317.

World Health Organization, 2021. WHO Global Air Quality Guidelines: Particulate Matter (PM2.5 and PM10), Ozone, Nitrogen Dioxide, Sulfur Dioxide and Carbon Monoxide. WHO, Geneva.